Cell Reports
Report

Specific DNA-RNA Hybrid Recognition by TAL Effectors

Ping Yin,[1,3,5] Dong Deng,[1,3,5] Chuangye Yan,[2,3] Xiaojing Pan,[1,3] Jianzhong Jeff Xi,[4] Nieng Yan,[1,3] and Yigong Shi[2,3,*]
[1]State Key Laboratory of Bio-membrane and Membrane Biotechnology
[2]Ministry of Education Key Laboratory of Protein Science
[3]Tsinghua-Peking Joint Center for Life Sciences, Center for Structural Biology, School of Life Sciences and School of Medicine
Tsinghua University, Beijing 100084, China
[4]Department of Biomedical Engineering, College of Engineering, Peking University, Beijing 100871, China
[5]These authors contributed equally to this work
*Correspondence: shi-lab@tsinghua.edu.cn
http://dx.doi.org/10.1016/j.celrep.2012.09.001

SUMMARY

The transcription activator-like (TAL) effector targets specific host promoter through its central DNA-binding domain, which comprises multiple tandem repeats (TALE repeats). Recent structural analyses revealed that the TALE repeats form a superhelical structure that tracks along the forward strand of the DNA duplex. Here, we demonstrate that TALE repeats specifically recognize a DNA-RNA hybrid where the DNA strand determines the binding specificity. The crystal structure of a designed TALE in complex with the DNA-RNA hybrid was determined at a resolution of 2.5 Å. Although TALE repeats are in direct contact with only the DNA strand, the phosphodiester backbone of the RNA strand is inaccessible by macromolecules such as RNases. Consistent with this observation, sequence-specific recognition of an HIV-derived DNA-RNA hybrid by an engineered TALE efficiently blocked RNase H-mediated degradation of the RNA strand. Our study broadens the utility of TALE repeats and suggests potential applications in processes involving DNA replication and retroviral infections.

INTRODUCTION

Transcription activator-like effectors (TALEs) are secreted by phytopathogenic bacteria of the genus *Xanthomonas* and injected into host cells through the type III secretion system (Bai et al., 2000; Boch and Bonas, 2010; Bonas et al., 1993; Gu et al., 2005; Swarup et al., 1992; White and Yang, 2009), where they modulate transcription through direct DNA binding (Kay et al., 2007; Romer et al., 2007). The code of DNA recognition by the variable diresidue (RVD) in each TALE repeat has been identified through both experimental and bioinformatic approaches (Boch et al., 2009; Moscou and Bogdanove, 2009). The bases A, G, C, and T can be recognized by the RVDs NI (Asn-Ile), NN (Asn-Asn), HD (His-Asp), and NG (Asn-Gly), respectively (Boch and Bonas, 2010). The modular assembly of TALE repeats provides an important tool for genome manipulation (Bogdanove and Voytas, 2011; McMahon et al., 2012; Reyon et al., 2012). Customized TALE nucleases (known as TALEN) have been generated to target specific genes in yeast (Christian et al., 2010), worm (Wood et al., 2011), and zebrafish (Huang et al., 2011), as well as to engineer human pluripotent cells (Hockemeyer et al., 2011).

The crystal structures of TALE-DNA complexes (Deng et al., 2012a; Mak et al., 2012) reveal that the second residue of an RVD directly contacts a DNA base, whereas the first residue stabilizes the conformation of the RVD loop. Notably, in the TALE-bound double-stranded DNA (dsDNA), the bases as well as the backbone phosphates in the forward strand (sense strand), but not in the reverse strand (antisense strand), are specifically recognized by RVDs in TALE repeats (Figures 1A and S1A) (Deng et al., 2012a). This structural observation suggests that the reverse DNA strand might be dispensable for TALE binding. Thus, we speculated that TALE might be able to recognize single-stranded DNA (ssDNA) or a DNA-RNA hybrid in which the DNA is the forward strand. In this report, we have combined structural biology and biochemical approaches to demonstrate that TALE repeats can specifically recognize the DNA-RNA hybrid where the DNA strand determines the binding specificity. Furthermore, designed TALE repeats can specifically protect the target DNA-RNA hybrids from degradation by RNase H. The discoveries presented here suggest potential applications of TAL effectors in the modulation of biological processes involving the maintenance and degradation of DNA-RNA hybrids such as DNA replication and retroviral infections.

RESULTS AND DISCUSSION

TALE Repeats of dHax3 Specifically Recognize a DNA-RNA Hybrid

The 12 TALE repeats of dHax3, a designed TALE (Deng et al., 2012a; Mahfouz et al., 2011), bind to the target dsDNA with a dissociation constant of approximately 0.3 μM, as estimated by results of the electrophoretic mobility shift assay (EMSA) (Figure 1B, lanes 1–5; Figure S1B, lanes 1–11). To examine whether TAL effectors can bind to nucleic acids other than dsDNA, we assessed the binding of dHax3 to ssDNA, a DNA-RNA hybrid, ssRNA, and dsRNA. In contrast to the specific binding with its target dsDNA (Figure 1B, lanes 1–5), dHax3 exhibited little

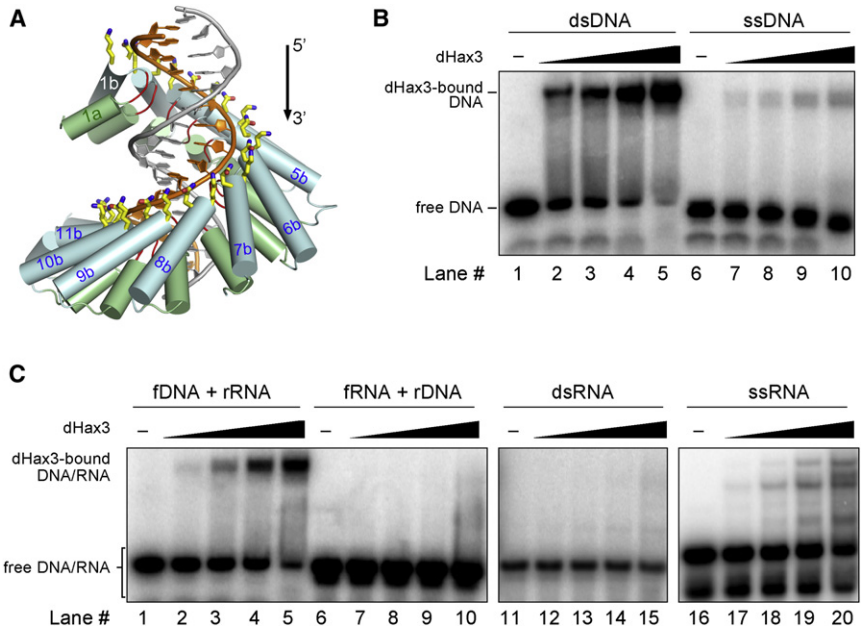

Figure 1. The TALE Repeats of dHax3 Specifically Recognize a DNA-RNA Hybrid

(A) Only the forward DNA strand is in direct contact with the TALE repeats. Shown here is a schematic representation of the dHax3-dsDNA complex (Deng et al., 2012a). The forward and reverse DNA strands are colored gold and gray, respectively. The two residues in each repeat that contact the DNA phosphates are shown as yellow sticks. The RVD loops are colored red. See also Figure S1A.

(B) dHax3 exhibits little binding for ssDNA. Details of EMSA are described in the Experimental Procedures. dHax3 concentrations were 0, 0.15, 0.44, 1.33, and 4 μM, respectively, in lanes 1–5 and 6–10. The probe concentration was approximately 4 nM in each lane. The same range of concentrations was applied to the assays in (C). See also Figure S1B.

(C) dHax3 specifically recognizes the DNA-RNA hybrid with forward DNA strand (lanes 1–5). f, forward strand; r, reverse strand. dHax3 showed no apparent binding to the DNA-RNA hybrid with reverse DNA strand (lanes 6–10) or dsRNA (lanes 11–15). dHax3 displayed weak binding to ssRNA (lanes 16–20). The free ssRNA contains a major band and a minor band on the gel (lane 16)—most likely a consequence of secondary structure formation (because this ssRNA is homogeneous on denaturing PAGE gel). All structural figures were prepared with PyMol (DeLano, 2002).

specific binding to the forward DNA strand alone (ssDNA) (Figure 1B, lanes 6–10) or a mutated dHax3 binding sequence in which six T bases were replaced by C bases (Figure S1B, lanes 12–22). This result suggests that the presence of the reverse strand may be essential for recognition of the forward DNA strand by TALE, perhaps for maintenance of appropriate base conformation in the forward DNA strand.

Next, we examined whether either strand of the dsDNA can be replaced by RNA for binding to dHax3. The DNA-RNA hybrid, with RNA as the reverse strand, retained specific binding to dHax3; the dissociation constant has been moderately reduced to about 1 μM (Figure 1C, lanes 1–5; data not shown). In contrast, the reciprocal DNA-RNA hybrid, with RNA as the forward strand, led to complete abrogation of dHax3 binding (Figure 1C, lanes 6–10). This finding suggests that RNA bases in the forward strand may not have the correct conformation for binding to dHax3. Consistent with this analysis, dsRNA also exhibited no specific binding to dHax3 (Figure 1C, lanes 11–15). Surprisingly, however, the forward RNA strand alone (ssRNA) appeared to retain some weak binding to dHax3 (Figure 1C, lanes 15–20). We speculate that the conformational flexibility of ssRNA allows some bases to adopt appropriate conformation for recognition by dHax3.

Crystal Structure of dHax3 TALE Repeats Bound to the DNA-RNA Hybrid

Compared to B-form dsDNA, the free DNA-RNA hybrid exhibits a different conformation, closely resembling that of the A-form dsDNA (Gyi et al., 1998; Shaw and Arya, 2008; Shi and Berg, 1995). To understand how dHax3 can specifically recognize the DNA-RNA hybrid, we crystallized dHax3 in complex with a 17 bp DNA-RNA hybrid in the space group $P6_1$. This space group, with one dHax3-DNA-RNA complex in each asymmetric unit, is different from that of the dHax3-dsDNA complex (Deng et al., 2012a). The structure was determined by molecular replacement using atomic coordinates of the dsDNA-bound dHax3 (PDB accession code 3V6T) (Deng et al., 2012a) and was refined to a resolution of 2.5 Å (Figure 2, Table S1). The presence of the reverse RNA strand is clearly identified by a string of discrete and strong electron densities that are associated with the 2′ oxygen atoms in the RNA oxyribose (Figure S2).

The overall structure of the dHax3-DNA-RNA hybrid is similar to that of the dHax3-dsDNA complex (Deng et al., 2012a) (Figure S3A). The structure of dHax3 bound to the DNA-RNA hybrid can be superimposed to that of the dsDNA-bound dHax3 with a root-mean-squared deviation (RMSD) of 0.77 Å over 441 Cα atoms (Figure S3B). Similar to the dHax3-bound dsDNA (Deng et al., 2012a), the dHax3-bound DNA-RNA hybrid also exhibits a distorted B-form conformation, with 11 bp per helical turn and a longer pitch compared to the B-form DNA duplex (Figure S3C, Table S2). The forward DNA strands in these two complexes have a nearly identical conformation in all but three nucleotides at the 3′ end (Figure S3D). Superposition of the DNA-RNA hybrid with the dsDNA reveals significant backbone shift in the reverse strand (Figure S3E). The positions of the phosphate groups are different by as much as 0.7 Å in the middle stretch and 4.8 Å at both ends of the strand. Furthermore, we believe that such conformational flexibility of the reverse strands, initially observed in the structure of the dHax3-dsDNA complex (Deng et al., 2012a), may play an important role in allowing specific recognition of the forward DNA strand. Notably, the 2′ hydroxyl groups of RNA, which represent the sole chemical

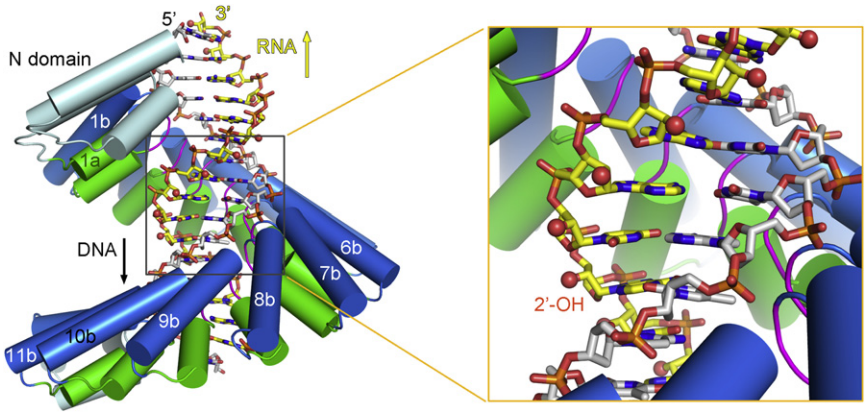

Figure 2. Crystal Structure of the Complex between dHax3 and the DNA-RNA Hybrid

The superhelical assembly of dHax3 (residues 231–720) binds to the major groove of the DNA-RNA hybrid. dHax3 contains 11.5 repeats. The flanking N- and C-terminal helices are shown in cyan. An enlarged view is shown on the right. Note that the 2′-hydroxyl groups of each nucleotide in the RNA strand, shown in red spheres, are located in the minor groove and away from the RVDs of TALE repeats.

See also Figure S2, Figure S3, and Table S1.

difference between RNA and DNA, point away from the protein and are completely exposed to solvent (Figure 2). This observation is fully consistent with the tolerance of both DNA and RNA in the reverse strand for binding to TALE.

TALE Repeats Protect Specific DNA-RNA Hybrids from RNase H Degradation

Despite a lack of direct interactions, the backbone phosphate groups in the RNA strand of the DNA-RNA hybrid are in close proximity to the TALE repeats (Figure 3A). Among the 12 nucleotides of the RNA strand that are complementary to the DNA-recognition sequence, the ones corresponding to positions 3–12 are partially "wrapped" by the TALE repeats (Figure 3A), most likely making these nucleotides inaccessible to bulky moiety such as a protein or enzyme. Given the fact that RNase H cleaves the RNA strand of the DNA-RNA hybrid by attacking the 3′ O-P bond (Tramontano and Di Santo, 2010), our observed structural feature suggests that dHax3 may be able to protect the RNA strand from degradation by RNase H. To test this hypothesis, we designed an RNase H protection assay, in which the substrate was generated between a ^{32}P-labeled 49 nt RNA and a 31 nt DNA that contains the dHax3-recognition sequence (Figure 3B). This design leaves an 18 nt 5′ overhang in the RNA sequence, which allows convenient detection after RNase H degradation.

In the absence of dHax3, the RNA sequence annealed to the DNA strand was digested by RNase H, yielding a specific cleavage pattern (Figure 3B, lane 3). The ribonuclease T1, known to specifically cleave after the base G, was employed to generate a reference ladder (Figure 3B, lane 13). Comparison of these two cleavage patterns revealed that the main cleavage products of the RNA strand, comprising four closely spaced bands, are those from the 5′ end to the sequence UAAA within the dHax3-binding site. In sharp contrast to the cleavage pattern generated in the absence of dHax3, the quadruplet cleavage products of the RNA strand gradually disappeared in response to increasing concentrations of the dHax3 protein (Figure 3B, lanes 3–10). Approximately half of the cleavage activity was blocked in the presence of 60 nM dHax3 (Figure 3B, lane 6). Concomitantly, novel cleavage products of the RNA strand appeared in the presence of dHax3. These cleavage products contain 5–12 more nucleotides than those found in the absence of dHax3, indicating that dHax3 not only shielded its binding sequence from RNase H degradation but also extended the protection to extra nucleotides, most likely because of steric clash between the N-terminal domain of dHax3 and RNase H.

To further corroborate the concept that binding of the DNA-RNA hybrid by TALE protects against degradation by RNase H, we extended the dHax3-binding sequence by 12 nucleotides (5′-CTCCAGCTCGAG-3′) and examined whether a designed TALE protein could protect the complementary RNA strand (Figure 3C). On the basis of the dHax3 scaffold, we engineered a TALE protein with 23.5 repeats (TALE24), which would recognize the combined 24 nt DNA sequence containing the dHax3-binding sequence and 5′-CTCCAGCTCGAG-3′ (Tables S3 and S5) in addition to an obligatory base T at position 0 (Boch et al., 2009; Moscou and Bogdanove, 2009). In the absence of TALE24, RNase H degraded the DNA-RNA hybrid to smaller cleavage products in comparison to those seen in Figure 3B (Figure 3C, lane 3). This result is consistent with the fact that the DNA-RNA hybrid contains a shortened ssRNA overhang in comparison to that seen in Figure 3B. In the presence of increasing concentrations of TALE24, these cleavage products gradually faded and novel, longer cleavage fragments appeared (Figure 3C, lanes 4–10). Comparison with the T1 control revealed that the entire 25 nt RNA sequence and its vicinity are protected from RNase H degradation.

A Designed TALE Protein Protects an HIV-Specific DNA-RNA Hybrid from RNase H Degradation

The finding that TALE repeats protect the DNA-RNA hybrid from RNase H degradation suggests potential application in fighting retroviruses through the control of reverse transcription, because RNase H-mediated degradation of the RNA template after synthesis of complementary DNA is indispensible for the replication of retroviruses (Basu et al., 2008; Sarafianos et al., 2009). Blockage of RNA degradation, perhaps by a designed TALE, may represent a novel approach in antiviral therapies.

On the basis of the dHax3 scaffold, we designed a 22.5-repeat TALE protein, named TALE$_{HIV}$ (Table S4), to specifically recognize a 23 nt sequence element in addition to a preceding base T of the reverse transcription product of the HIV genome at its 5′ repeat region (Figure 4, Table S5). TALE$_{HIV}$ was purified to approximately 95% homogeneity, and a DNA-RNA hybrid was prepared with a 12 nt overhang (Figure 4). In the absence of TALE$_{HIV}$, the RNA strand of the DNA-RNA hybrid was degraded

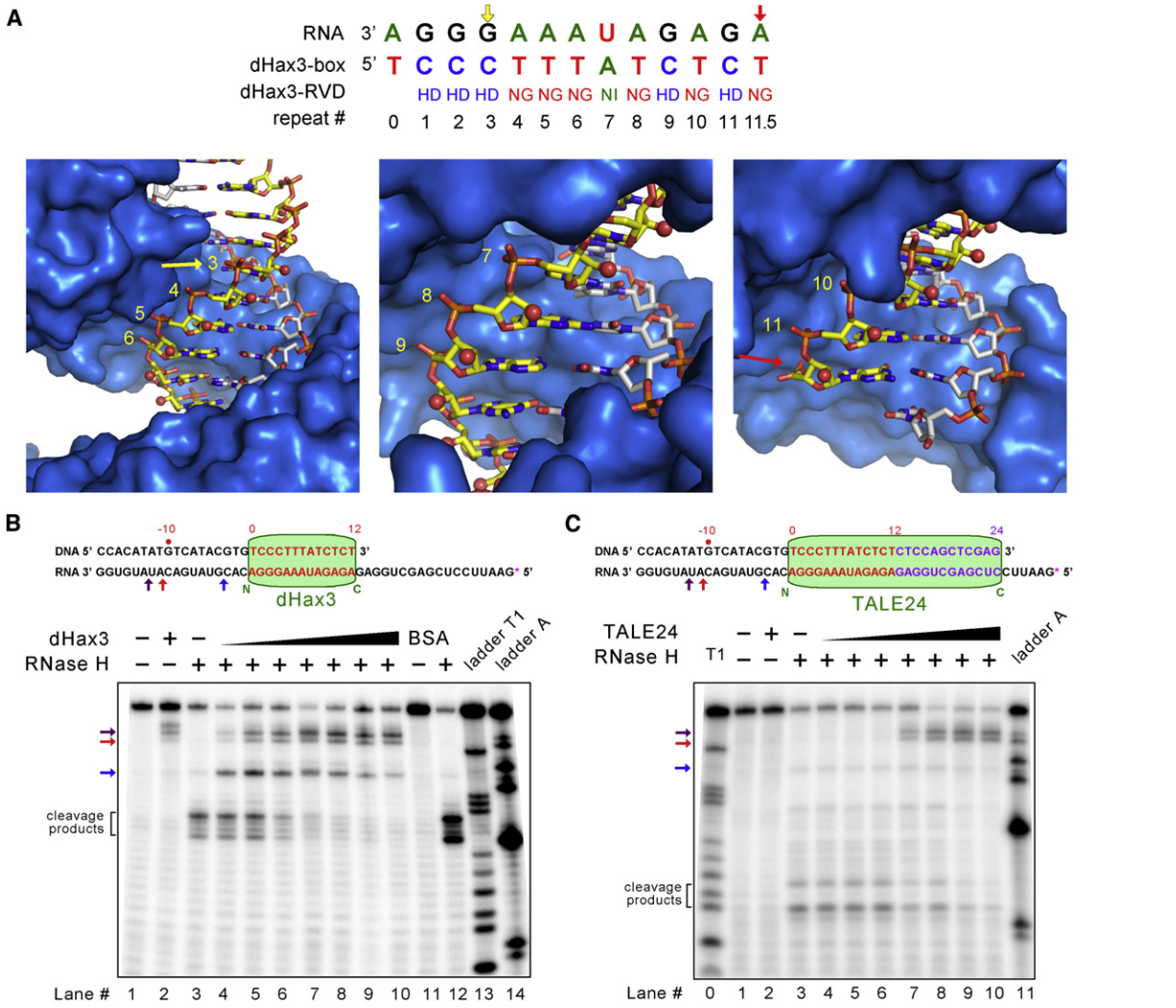

Figure 3. TALE Repeats Protect Specific DNA-RNA Hybrids from RNase H Degradation

(A) The phosphodiester backbone of the RNA strand in the DNA-RNA hybrid is in close proximity to the TALE repeats. Shown are the recognition sequences of the DNA-RNA hybrid by dHax3. The nucleotide numbers in the DNA strand correspond to numbers labeled on the structure in the lower three panels.

(B) dHax3 protects a specific DNA-RNA hybrid from RNase H degradation. Shown in the upper panel are sequences of the DNA-RNA hybrid. RNA is ^{32}P-labeled at the 5′ end, indicated by a red asterisk. The final concentrations of dHax3 were 0.004, 0.015, 0.06, 0.25, 1, 4, and 16 μM, respectively, in lanes 4–10. BSA was added at a final concentration of 16 μM (lanes 11 and 12). "ladder T1" and "ladder A" refer to the cleavage of the ssRNA by RNase T1 and RNase A, respectively.

(C) A designed TALE protein protects the 24 nt (excluding the base T at position 0) DNA-RNA hybrid from RNase H degradation. The final concentrations of TALE24 were 0.0004, 0.0015, 0.006, 0.025, 0.1, 0.4, and 1.6 μM, respectively, in lanes 4–10.

See also Tables S3 and S5.

to yield two prominent cleavage products by RNase H (Figure 4, lane 3). In the presence of increasing amounts of $TALE_{HIV}$, these cleavage products gradually disappeared (Figure 4, lanes 4–10), indicating protection. At a concentration of 6 nM, $TALE_{HIV}$ blocked at least 50% of RNase H-mediated degradation of the RNA strand (Figure 4, lane 6). The specificity is manifested in the observations that BSA was unable to protect this specific HIV RNA element from RNase H degradation and TALE24 exhibited very limited protection at a concentration of 1.6 μM, the latter most likely due to nonspecific binding (Figure 4, lanes 11–14).

Perspective

Many additional experiments, both in cells and in animal models, should be conducted in order to validate the concept that the binding of the DNA-RNA hybrid by TALEs may find clinical application. Notably, zinc finger proteins have been shown to specifically recognize DNA-RNA hybrids (Shi and Berg, 1995), and the endonuclease Fok I fused to zinc finger protein has been shown to cleave a DNA-RNA hybrid (Kim et al., 1997). However, it remains to be seen whether zinc finger proteins can be applied successfully for direct clinical benefits. Nevertheless, our finding that designed TALE repeats can

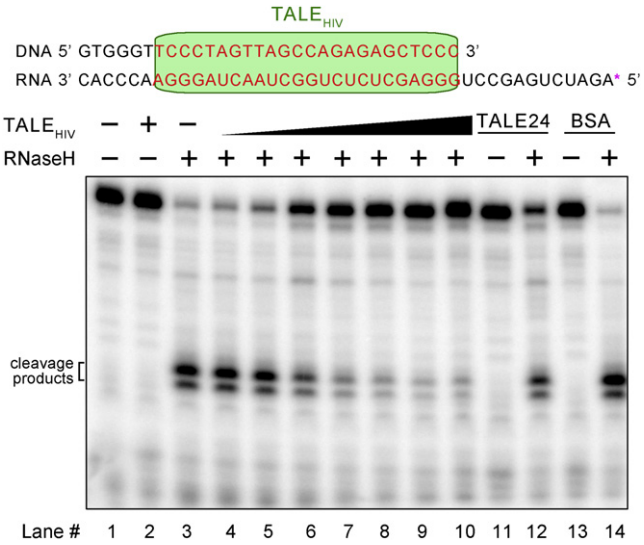

Figure 4. A Designed TALE Protein Protects an HIV-Specific DNA-RNA Hybrid from RNase H Degradation

The TALE protein, designated TALE$_{HIV}$, contains 22.5 tandem repeats. TALE$_{HIV}$ efficiently protected against RNase H-mediated degradation of a DNA-RNA hybrid that mimics the HIV replication intermediate. The final concentrations of TALE$_{HIV}$ were 0.0004, 0.0015, 0.006, 0.025, 0.1, 0.4, and 1.6 μM, respectively, in lanes 4–10. BSA (lanes 11 and 12) and TALE24 (lanes 13 and 14) were added at a final concentration of 1.6 μM each.

See also Tables S4 and S5.

protect the target RNA sequence of a DNA-RNA hybrid against RNase H degradation offers an additional exciting opportunity for consideration of potential therapeutic intervention against HIV and other retroviruses. DNA-RNA hybrids are associated not just with retroviruses but also with transcription in general and with DNA replication in which Okazaki fragments form to complete synthesis of the lagging DNA strand (Shaw and Arya, 2008). Binding of these specific DNA-RNA hybrids by designed TALEs may offer unprecedented opportunities for manipulation of these biochemical processes, and perhaps for disease intervention. Thus, our finding that TALE is able to specifically recognize a DNA-RNA hybrid, together with the recent report that TALE binds to methylated DNA sequences (Deng et al., 2012b), may greatly expand the utility and application of TALE. The hallmark property of TALEs, recognizing only a single DNA strand of the DNA-RNA hybrid, facilitates the design of such TALE proteins.

EXPERIMENTAL PROCEDURES

Vectors and Constructs

The cDNAs for the TALE tandem repeats were synthesized (View Solid Biotechnology). The sequences of DNA elements and proteins are shown in Tables S3–S5. In brief, for generation of TALE24 and TALE$_{HIV}$, SpeI and SalI cuttings sites were introduced at the ends of the synthesized cDNA for these TALE repeats. The cDNA encoding dHax3 was subcloned into pET-21b (Novagen) (Deng et al., 2012a). The cutting sites for NheI and SalI were introduced into dHax3 cDNA such that the fragment encoding the 12 repeats can be replaced by the cDNA encoding the 24 repeats of TALE24 or TALE$_{HIV}$.

Protein Expression and Purification

Plasmids encoding the engineered TALE proteins were transformed into *E. coli* Rosetta (DE3). Overexpression of TALEs was induced by 0.2 mM isopropyl -D-thiogalactoside (IPTG) when the optical density of cell culture at 600 nm (OD600) reached 0.8. After growth at 22°C for 16 hr, the cells were harvested and homogenized in the buffer containing 25 mM Tris-HCl (pH 8.0) and 500 mM NaCl. After sonication and centrifugation, the supernatant was applied to Ni^{2+} affinity resin (Ni-NTA, QIAGEN), followed by heparin affinity column (Heparin Sepharose 6 Fast Flow, GE Healthcare) and gel filtration chromotography (Superdex-200 10/30, GE Healthcare). The buffer for gel filtration contained 25 mM Tris-HCl (pH 8.0), 150 mM NaCl, and 10 mM DTT. Peak fractions from gel filtration were collected. Truncated dHax3 (residues 231–720) was purified as previously described (Deng et al., 2012a).

Crystallization

The synthesized forward DNA strand and the reverse RNA strand were mixed with equal molar amounts, heated at 85°C for 3 min, and annealed by slow cooling to 22°C over a period of 5 hr. For crystallization, dHax3 (residues 231∼720) and the 17 bp DNA-RNA hybrid were mixed with a molar ratio of approximately 1:1.5 at 4°C for 30 min. The DNA-RNA hybrid sequences are as follows: fDNA, 5′-TGTCCCTTTATCTCTCT-3′; rRNA, 5′-AGAGAGA UAAAGGGA CA-3′.

Crystals of the protein in complex with the DNA-RNA hybrid were grown at 18°C by the hanging-drop vapor-diffusion method. The crystals grew to full size overnight in the mother solution containing 11% PEG3350 (w/v), 12% ethanol, and 0.1 M MES (pH 6.3). But the diffraction of these crystals is too poor for data collection. Aging and dehydration strategies were applied to the crystals. We left the crystals in the incubator for aging from 2 days to 3 weeks. Then dehydration was applied faithfully according to the protocols described by Heras and Martin (2005). Eventually, one crystal diffracted X-rays to 2.5 Å resolution at the Shanghai Synchrotron Radiation Facility (SSRF) beam line BL17U after a 2 week aging followed by dehydration.

Data Collection and Structural Determination

All data sets were integrated and scaled with the HKL2000 (Otwinowski and Minor, 1997) package. Further processing was carried out with programs from the CCP4 suite (Collaborative Computational Project, 1994). The structure of dHax3 in complex with the DNA-RNA hybrid was determined by molecular replacement with the structure of dHax3 bound to dsDNA (PDB accession code 3V6T) used as the initial search model in the program PHASER (McCoy et al., 2007). The structure was refined with PHENIX (Adams et al., 2002) and COOT (Emsley and Cowtan, 2004) iteratively. Data collection and structural refinement statistics are summarized in Table S1.

EMSA

The single-stranded DNA or RNA oligonucleotides were radiolabeled at the 5′ end with [γ-^{32}P] ATP (5,000 Ci/mmol; Furui Biotech, Beijing, China) with the use of T4 polynucleotide kinase (Takara). The sequences of nucleic acid oligos used in EMSA are as follows:

fRNA, 5′-CCACAUAUGUCAUACGUGUCCCUUUAUCUCUCUCCAGCUC GAGGAAUUC-3′;
rRNA, 5′-GAAUUCCUCGAGCUGGAGAGAGAUAAAGGGACACGUAUGA CAUAUGUGG-3′;
fDNA, 5′-CCACATATGTCATACGTGTCCCTTTATCTCTCTCCAGCTCGAG GAATTC-3′;
rDNA, 5′-GAATTCCTCGAGCTGGAGAGAGATAAAGGGACACGTATGAC ATATGTGG-3′

The dsDNA, DNA-RNA hybrid, and dsRNA were generated by mixing equal molar quantities of forward and reverse strands. For EMSA, TALE proteins with indicated concentrations were incubated with approximately 4 nM ^{32}P-labeled probe on ice in the binding buffer containing 20 mM Tris-HCl (pH 8.0), 50 mM NaCl, 5 mM $MgCl_2$, 5% glycerol (w/v), 50 ng/μl poly (dI·dC), and 0.1 mg/ml bovine serum albumin (BSA) for 20 min. Reactions were then resolved on 6% native acrylamide gels (37.5:1 for acrylamide: bisacrylamide) in 0.25× Tris

borate buffer under an electric field of 15 V/cm for 1 hr. Vacuum-dried gels were exposed to phosphorimager screens and analyzed by a Typhoon Trio variable scanner (Amersham Pharmacia).

RNase H Protection Assay

Generation of the DNA-RNA probes was described above. TALE proteins or BSA were incubated with approximately 5 nM ^{32}P-labeled probes for 20 min on ice in a final volume of 20 μl in the RNase H reaction buffer containing 20 mM Tris-HCl (pH 8.0), 50 mM NaCl, 5 mM $MgCl_2$, and 10 mM DTT. For each reaction, 5 μl 0.1 U/μl RNase H (Takara) was added to the reaction mixture and incubated for 5 min at room temperature. Reactions were quenched by the addition of phenol-chloroform, followed by ethanol precipitation. Finally, the samples were resuspended in RNA-loading buffer (95% formamide, 18 mM EDTA, 0.025% xylene cyanol, 0.025% bromophenol blue) and applied to a 12% denaturing (7 M urea) polyacrylamide gel in 1× tris-borate-EDTA (TBE) buffer under an electric field of 15 V/cm for 2 hr. Vacuum-dried gels were exposed to phosphorimager screens and analyzed with a Typhoon Trio variable scanner (Amersham Pharmacia). The ladders were generated by incubating RNase T1 or RNase A with the ssRNA probe at room temperature for 10 min.

ACCESSION NUMBERS

The Protein Data Bank accession number for the atomic coordinates and structural factors is 4GG4.

SUPPLEMENTAL INFORMATION

Supplemental Information includes three figures and five tables and can be found with this article online at http://dx.doi.org/10.1016/j.celrep.2012.09.001.

LICENSING INFORMATION

ACKNOWLEDGMENTS

We thank J. He and Q. Wang at the Shanghai Synchrotron Radiation Facility (SSRF) beam line BL17U. This work was supported by funds from the Ministry of Science and Technology (grant numbers 2009CB918801, 2011CB910501, and 2009CB918802), projects 30888001, 91017011, and 31070644 of the National Natural Science Foundation of China, and the Commission of Science and Technology of Beijing.

Received: June 15, 2012
Revised: August 8, 2012
Accepted: September 10, 2012
Published online: September 27, 2012

REFERENCES

Adams, P.D., Grosse-Kunstleve, R.W., Hung, L.W., Ioerger, T.R., McCoy, A.J., Moriarty, N.W., Read, R.J., Sacchettini, J.C., Sauter, N.K., and Terwilliger, T.C. (2002). PHENIX: building new software for automated crystallographic structure determination. Acta Crystallogr. D Biol. Crystallogr. *58*, 1948–1954.

Bai, J., Choi, S.H., Ponciano, G., Leung, H., and Leach, J.E. (2000). Xanthomonas oryzae pv. oryzae avirulence genes contribute differently and specifically to pathogen aggressiveness. Mol. Plant Microbe Interact. *13*, 1322–1329.

Basu, V.P., Song, M., Gao, L., Rigby, S.T., Hanson, M.N., and Bambara, R.A. (2008). Strand transfer events during HIV-1 reverse transcription. Virus Res. *134*, 19–38.

Boch, J., and Bonas, U. (2010). Xanthomonas AvrBs3 family-type III effectors: discovery and function. Annu. Rev. Phytopathol. *48*, 419–436.

Boch, J., Scholze, H., Schornack, S., Landgraf, A., Hahn, S., Kay, S., Lahaye, T., Nickstadt, A., and Bonas, U. (2009). Breaking the code of DNA binding specificity of TAL-type III effectors. Science *326*, 1509–1512.

Bogdanove, A.J., and Voytas, D.F. (2011). TAL effectors: customizable proteins for DNA targeting. Science *333*, 1843–1846.

Bonas, U., Conrads-Strauch, J., and Balbo, I. (1993). Resistance in tomato to Xanthomonas campestris pv vesicatoria is determined by alleles of the pepper-specific avirulence gene avrBs3. Mol. Gen. Genet. *238*, 261–269.

Christian, M., Cermak, T., Doyle, E.L., Schmidt, C., Zhang, F., Hummel, A., Bogdanove, A.J., and Voytas, D.F. (2010). Targeting DNA double-strand breaks with TAL effector nucleases. Genetics *186*, 757–761.

Collaborative Computational Project, Number 4. (1994). The CCP4 suite: programs for protein crystallography. Acta Crystallogr. D Biol. Crystallogr. *50*, 760–763.

DeLano, W.L. (2002). The PyMOL Molecular Graphics System. on World Wide Web http://wwwpymolorg.

Deng, D., Yan, C., Pan, X., Mahfouz, M., Wang, J., Zhu, J.K., Shi, Y., and Yan, N. (2012a). Structural basis for sequence-specific recognition of DNA by TAL effectors. Science *335*, 720–723.

Deng, D., Yin, P., Yan, C., Pan, X., Gong, X., Qi, S., Xie, T., Mahfouz, M., Zhu, J.K., Yan, N., and Shi, Y. (2012b). Recognition of methylated DNA by TAL effectors. Cell Res. Published Septmeber 4, 2012. http://dx.doi.org/10.1038/cr.2012.127.

Emsley, P., and Cowtan, K. (2004). Coot: model-building tools for molecular graphics. Acta Crystallogr. D Biol. Crystallogr. *60*, 2126–2132.

Gu, K., Yang, B., Tian, D., Wu, L., Wang, D., Sreekala, C., Yang, F., Chu, Z., Wang, G.L., White, F.F., and Yin, Z. (2005). R gene expression induced by a type-III effector triggers disease resistance in rice. Nature *435*, 1122–1125.

Gyi, J.I., Lane, A.N., Conn, G.L., and Brown, T. (1998). Solution structures of DNA.RNA hybrids with purine-rich and pyrimidine-rich strands: comparison with the homologous DNA and RNA duplexes. Biochemistry *37*, 73–80.

Heras, B., and Martin, J.L. (2005). Post-crystallization treatments for improving diffraction quality of protein crystals. Acta Crystallogr. D Biol. Crystallogr. *61*, 1173–1180.

Hockemeyer, D., Wang, H., Kiani, S., Lai, C.S., Gao, Q., Cassady, J.P., Cost, G.J., Zhang, L., Santiago, Y., Miller, J.C., et al. (2011). Genetic engineering of human pluripotent cells using TALE nucleases. Nat. Biotechnol. *29*, 731–734.

Huang, P., Xiao, A., Zhou, M., Zhu, Z., Lin, S., and Zhang, B. (2011). Heritable gene targeting in zebrafish using customized TALENs. Nat. Biotechnol. *29*, 699–700.

Kay, S., Hahn, S., Marois, E., Hause, G., and Bonas, U. (2007). A bacterial effector acts as a plant transcription factor and induces a cell size regulator. Science *318*, 648–651.

Kim, Y.G., Shi, Y., Berg, J.M., and Chandrasegaran, S. (1997). Site-specific cleavage of DNA-RNA hybrids by zinc finger/FokI cleavage domain fusions. Gene *203*, 43–49.

Mahfouz, M.M., Li, L., Shamimuzzaman, M., Wibowo, A., Fang, X., and Zhu, J.K. (2011). De novo-engineered transcription activator-like effector (TALE) hybrid nuclease with novel DNA binding specificity creates double-strand breaks. Proc. Natl. Acad. Sci. USA *108*, 2623–2628.

Mak, A.N., Bradley, P., Cernadas, R.A., Bogdanove, A.J., and Stoddard, B.L. (2012). The crystal structure of TAL effector PthXo1 bound to its DNA target. Science.

McCoy, A.J., Grosse-Kunstleve, R.W., Adams, P.D., Winn, M.D., Storoni, L.C., and Read, R.J. (2007). Phaser crystallographic software. J. Appl. Cryst. *40*, 658–674.

McMahon, M.A., Rahdar, M., and Porteus, M. (2012). Gene editing: not just for translation anymore. Nat. Methods *9*, 28–31.

Moscou, M.J., and Bogdanove, A.J. (2009). A simple cipher governs DNA recognition by TAL effectors. Science *326*, 1501.

Otwinowski, Z., and Minor, W. (1997). Processing of X-ray diffraction data collected in oscillation mode. Methods Enzymol. *276*, 307–326.

Reyon, D., Tsai, S.Q., Khayter, C., Foden, J.A., Sander, J.D., and Joung, J.K. (2012). FLASH assembly of TALENs for high-throughput genome editing. Nat. Biotechnol. *30*, 460–465.

Romer, P., Hahn, S., Jordan, T., Strauss, T., Bonas, U., and Lahaye, T. (2007). Plant pathogen recognition mediated by promoter activation of the pepper Bs3 resistance gene. Science *318*, 645–648.

Sarafianos, S.G., Marchand, B., Das, K., Himmel, D.M., Parniak, M.A., Hughes, S.H., and Arnold, E. (2009). Structure and function of HIV-1 reverse transcriptase: molecular mechanisms of polymerization and inhibition. J. Mol. Biol. *385*, 693–713.

Shaw, N.N., and Arya, D.P. (2008). Recognition of the unique structure of DNA:RNA hybrids. Biochimie *90*, 1026–1039.

Shi, Y., and Berg, J.M. (1995). Specific DNA-RNA hybrid binding by zinc finger proteins. Science *268*, 282–284.

Swarup, S., Yang, Y., Kingsley, M.T., and Gabriel, D.W. (1992). An Xanthomonas citri pathogenicity gene, pthA, pleiotropically encodes gratuitous avirulence on nonhosts. Mol. Plant Microbe Interact. *5*, 204–213.

Tramontano, E., and Di Santo, R. (2010). HIV-1 RT-associated RNase H function inhibitors: Recent advances in drug development. Curr. Med. Chem. *17*, 2837–2853.

White, F.F., and Yang, B. (2009). Host and pathogen factors controlling the rice-Xanthomonas oryzae interaction. Plant Physiol. *150*, 1677–1686.

Wood, A.J., Lo, T.W., Zeitler, B., Pickle, C.S., Ralston, E.J., Lee, A.H., Amora, R., Miller, J.C., Leung, E., Meng, X., et al. (2011). Targeted genome editing across species using ZFNs and TALENs. Science *333*, 307.